Rotational Fluctuations of Water inside the Nanopores of SBA-Type Molecular Sieves

Ligia Frunza,*,† Hendrik Kosslick,‡ Irene Pitsch,‡ Stefan Frunza,† and Andreas Schönhals§

National Institute of Materials Physics, R-077125 Bucharest-Magurele, Romania, Institute of Applied Chemistry, D-12489 Berlin, Germany, and Federal Institute of Materials Research and Testing, D-12205 Berlin, Germany

Received: December 3, 2004; In Final Form: March 7, 2005

The rotational molecular dynamics of water confined to nanoporous molecular sieves of a regular hexagonal (SBA-15) and of a foamlike pore structure was studied by dielectric spectroscopy in the frequency range from 10^{-2} to 10^{9} Hz and in a broad temperature interval. Two relaxation processes were observed: the process at lower frequencies is related to water molecules forming a layer, which is strongly adsorbed at the pore surface, whereas the relaxation process at higher frequencies is assigned to fluctuations of water molecules situated close to the center of the pore. The relaxation times of the low-frequency process for both materials and of the high-frequency process for the SBA-15 material have an unusual saddlelike temperature dependence, reported here for the first time. To describe this temperature dependence, a model developed for water confined to nanoporous glasses by Ryabov et al. [*J. Phys. Chem. B* **2001**, *105*, 1845] was applied, which considers two competing effects. The characteristic features of these two competing processes were compared with those reported for other porous systems.

Introduction

Molecular sieves with cylindrical pores and a hexagonally ordered structure (MCM-41, SBA-15)[1,2] or with other types of uniform large pores and a foamlike or a wormhole framework structure[2] were recently synthesized. Moreover, materials with a combined so-called micro- and mesoporosity were also obtained[3] having a higher thermal, hydrothermal, and mechanical stability. All these nanoporous materials can become important for applications as hosts for chemical sensors, in water separation processes, in catalytic reactions involving bulky molecules, such as those used in producing fine chemicals,[4] and in heterogenizing the homogeneous catalysts.[5] Detailed knowledge of the diffusion and more general of the molecular mobility of adsorbates in such porous materials is therefore essential. However, there are only a few papers dealing with the dynamical behavior of polar, low-molecular-weight adsorbates confined to MCM-41-type molecular sieves,[6−11] and very few results referring to SBA materials have been published so far.[8,12]

In this paper first results concerning the molecular mobility of water molecules confined to SBA-type nanoporous materials with a hexagonal or a cellular structure studied by dielectric spectroscopy in a broad frequency and temperature interval are presented. Two relaxation processes both assigned to fluctuations of water molecules located inside the pores were observed. A nonmonotonic saddlelike temperature dependence of the relaxation time was found, which is similar to that recently reported for water in certain porous glasses[13] or in sodalite cages of the Na−Y zeolite.[14] This behavior is explained using a model developed for water in porous glasses[15] and later found to be applicable to describe the relaxation kinetics in other cases such as confined liquid crystals, doped ferroelectric crystals, and heteropolymer folding.[16]

* Corresponding author. E-mail lfrunza@infim.ro.
† National Institute of Materials Physics.
‡ Institute of Applied Chemistry.
§ Federal Institute of Materials Research and Testing.

Experimental Section

Materials. Nanoporous molecular sieves were hydrothermally synthesized by using nonionic surfactants (poly(ethylene oxide)-*b*-poly(propylene oxide) block copolymers) as synthesis-directing agents and silica and aluminosilicate oligomer species.[17] The aluminum-containing molecular sieves were obtained under mild pH conditions.[18] The organic material was removed by calcination at 773 K in air.

The molecular sieves were routinely characterized by X-ray diffraction, nitrogen adsorption measurements, electron (scanning and transmission) microscopy, MAS NMR (^{29}Si, ^{27}Al, ^{1}H), thermogravimetric−differential thermal analysis (TG−DTA) measurements, and FTIR spectroscopy, as described in detail elsewhere.[17,19] The structure of the molecular sieves and their main characteristics are summarized in Table 1.

Transmission electron microscopy (TEM) images of these samples are given in Figure 1A,B. The sample AlSBA-15 (Figure 1A) shows the typical pattern of hexagonally arranged pores (channels), while a cellular structure is found for the sample NMS-F (Figure 1B).

Broadband Dielectric Measurements. For the dielectric measurements, the samples were prepared by pressing the powder of molecular sieves to pellets. Before the measurements, the samples were outgassed in a vacuum at 673 K for 12 h to remove water and organic impurities. Then the samples were kept in a desiccator up to the measurements. The dielectric experiments were not conducted in a closed cell: Thus, the effect of the hydration degree is not directly accessible. However, a filling factor Θ was estimated on the basis of the actual water uptake and the maximum pore filling to (less than) $\Theta = 0.1$.

Dielectric spectroscopy in a broad frequency range (10^{-2}−10^{9} Hz) was employed to study the molecular (rotational) dynamics of the confined water molecules. The complex dielectric function

$$\epsilon^*(f) = \epsilon'(f) - i\epsilon''(f) \quad (1)$$

10.1021/jp044503t CCC: $30.25 © 2005 American Chemical Society
Published on Web 04/02/2005

TABLE 1: Properties of the Nanoporous Molecular Sieves

sample	composn	structure	S_{BET} ($m^2\,g^{-1}$)	BJH pore diam (nm)	BJH V_{pores} ($cm^3\,g^{-1}$)	particle morphology by SEM
AlSBA-15	Si/Al = 13	hexagonal, cylindrical pores	602	8.4	0.95	1−10 μm rosette-like aggregates
NMS-F	Si	cellular (foamlike)	546	17.2	1.92	0.5−10 μm, different shapes

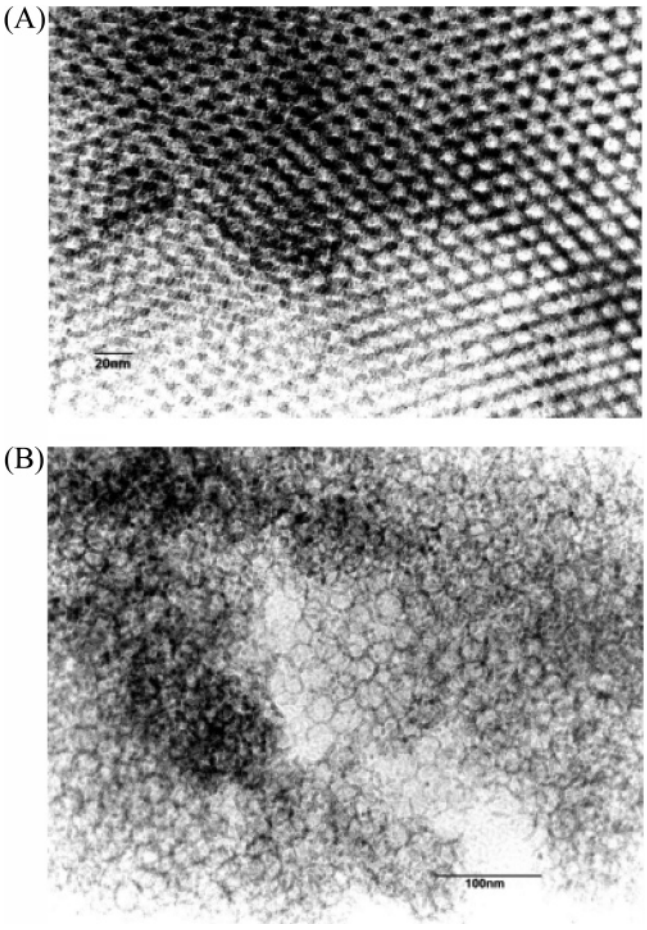

Figure 1. TEM images of the investigated molecular sieves: (A) AlSBA-15; (B) NMS-F.

(f, frequency; ϵ', real part; ϵ'', imaginary part) was measured using a Schlumberger frequency response analyzer FRA 1260 supplemented by a buffer amplifier of variable gain in the frequency range from 10^{-2} to 10^6 Hz and a coaxial line reflectometer based on a Hewlett-Packard impedance analyzer HP 4191 for high frequencies (10^6−10^9 Hz).[20] The temperature of the sample was controlled by nitrogen gas jet cryostats with a temperature stability better than 0.1 K. The investigations cover a temperature interval from 213 to 400 K.

To estimate the relaxation strength $\Delta\epsilon$ and the frequency at maximal loss f_p (further called relaxation rate) connected to the relaxation time τ by $f_p=1/(2\pi\tau)$, the model function of Havriliak−Negami (HN)[21]

$$\epsilon^*_{HN}(f) = \epsilon_\infty + \frac{\Delta\epsilon}{(1+(if/f_0)^\beta)^\gamma} \qquad (2)$$

(f_0 is a characteristic frequency close to f_p) was fitted to the data for each process. The fractional shape-parameters γ and β ($0 < \beta$, $\gamma\beta \leq 1$) describe the symmetric and asymmetric broadening of the relaxation spectra compared to a Debye relaxation function (for details see ref 21). If two relaxation peaks are observed in the frequency window, two HN functions were fitted simultaneously to the data. Conductivity contributions to the dielectric loss were described by σ/f^s, where σ is related to the dc conductivity of the sample and s ($0 < s \leq 1$) is a fitting parameter.[21]

Thermogravimetric Measurements. The water content c_w (in 1 g of dried molecular sieve) of the samples analyzed by dielectric spectroscopy was estimated by thermogravimetric measurements.[14] TG data were recorded with TG-DTA 92 (Setaram) equipment, working with a dried air flow at heating rates of 2 or 10 K min^{-1}. For comparison in all the TG experiments the same sample mass was used.

On the basis of the determined water content and by taking the density of confined water as $\rho_w^{conf} \approx 1$ g cm^{-3}, the filling factor of the pores $\Theta = c_w/(V_{pores}\rho_w^{conf})$ and the layer thickness of the confined water $h_w^{conf} = (c_w/\rho_w^{conf})/S_{BET}$ were roughly evaluated.

Results and Discussion

Dielectric Measurements. Water is a highly polar molecule. Hence, broadband dielectric spectroscopy is the method of choice to investigate its rotational fluctuations. The dielectric loss in the available frequency range measured for the two nanoporous molecular sieves, AlSBA-15 and NMS-F, is given in Figure 2 (A and B). Maxwell−Wagner−Sillars (MWS) effects (interface polarization phenomena due to charge separation processes) and a dc contribution are observed at low frequencies followed by a relaxation process (I) at higher frequencies. A further relaxation region (II) is observed for frequencies above 1 MHz.

The real and the imaginary parts of the dielectric function are related to each other by the Kramers−Kronig relationships, meaning that both quantities carry the same experimental information. Therefore the discussion will be further focused on the dielectric loss.

The frequency positions of both relaxation peaks in Figure 2 are separated by approximately 7 orders of magnitude. Because of this large separation, one might speculate that the low-frequency process is not related to water but for example, to the dry molecular sieve. However, it is well-known that in the experimental frequency and temperature window no relaxation process due to (dehydrated or empty) silica itself or to bulk liquid water molecules is expected.[22,23] Moreover it has been shown that the structurally related molecular sieve AlMCM-41 is rather a dielectrically inactive material:[10a] No relaxation process could be observed in the loss spectra in the relevant temperature range, and the real part of the dielectric function is constant in the whole frequency range.

It might be further argued that the mobility of the exchangeable cations contributes significantly to the dielectric signal as it is found for other molecular sieves.[24] But, one has to note that both materials have a negligible cation content: AlSBA-15 is in hydrogen form, whereas NMS-F is a pure silica. In fact, SBA-type molecular sieves behave like other related confining materials such as Anopore membranes and porous glass.[25−27]

One might also assign the low-frequency relaxation process to a Maxwell−Wagner−Sillars effect.[23,28] But, this interpretation might be ruled out because of the unusual temperature dependence of its characteristic frequencies as discussed below.

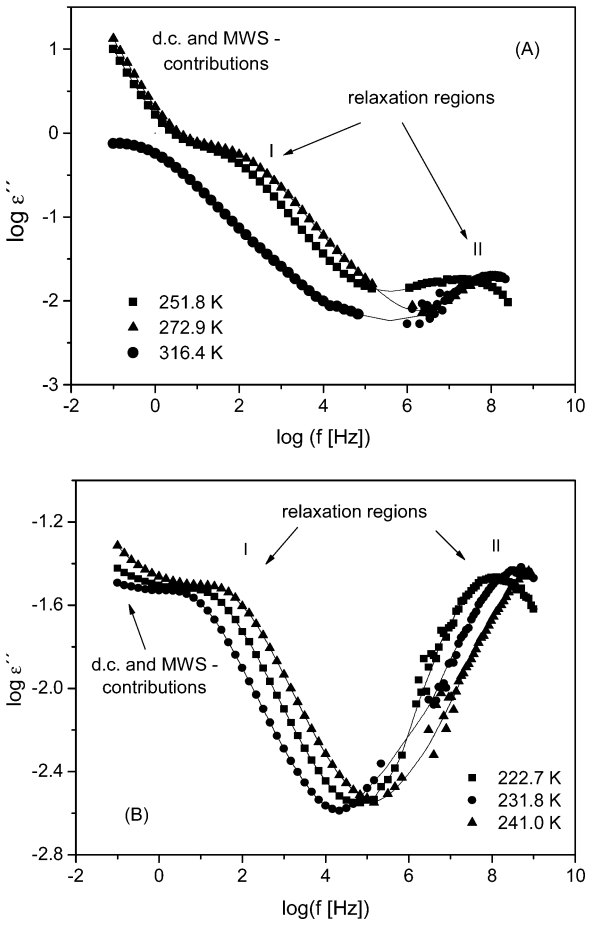

Figure 2. Dielectric loss vs frequency for the samples in the available frequency range at the indicated temperatures: (A) AlSBA-15 and (B) NMS-F containing water with a filling factor less than 0.1 (see the text). The lines are guides for the eyes.

Moreover the corresponding dielectric strength seems to be too small for such a mechanism.

Consequently, it was concluded that both observed relaxation processes should be assigned to the constrained rotational dynamics of water molecules confined in the nanopores. Moreover, these quite different dynamical properties reflect the existence of quite different water species. Different states of water confined to mesoporous systems were already confirmed by other investigations and methods. Using line shape analysis of ^{2}H double quantum filtered NMR and T_1 measurements for MCM-41 materials it was shown[9] that there are three different species of water having different dynamical properties. One species (species 1) has long reorientation times, and it is supposed that these water molecules are in close contact with the surface. The two other types of water molecules (species 2 and 3) have shorter reorientation times. The simplest model is to assume a layered structure of the water wherein the mobility of the molecules in these layers increases with increasing distance from the surface. A related model (an exchange between the molecules in different sites[16]) was discussed for some organic molecules confined to nanoporous glasses[29] and even for polymers.[30]

A similar picture of water in nanoporous Vycor glasses is given by Pissis et al.,[31] which performed dielectric measurements at room temperature and especially thermally stimulated dc and polarization investigations in a large temperature range. Two loss peaks were found: one peak at lower frequency (kHz−MHz) and a second one for frequencies above 1 GHz. These relaxation processes were assigned to the water molecules in a surface layer (restricted mobility) and to water molecules, which are located closer to the pore center. The actual values of the relaxation times depend on temperature and the filling degree of the pores. It is found that the relaxation rate increases with the filling factor.[31]

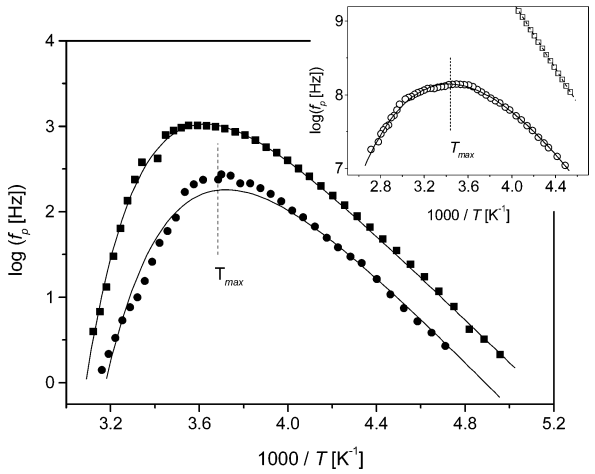

Figure 3. Relaxation rate f_p vs inverse temperature for relaxation process I in the low-frequency range: filled circles, AlSBA-15; filled squares, NMS-F. The lines are the fits of eq 3 to the data. The inset gives the relaxation rate f_p vs inverse temperature for relaxation process II in the high-frequency range: open circles, AlSBA-15; open squares, NMS-F. The line is the fit of eq 3 to the data for AlSBA-15. The dashed line is a fit of the Arrhenius equation to the data for NMS-F.

Also studies by neutron diffraction[14] of water in MCM-41 support this picture. In the presence of excess water, the pores are fully hydrated for their entire length. In partially filled samples the population density of water follows a radial function with a minimum on the pore center and a maximum near the wall. Moreover, differential scanning calorimetry data for water in SBA-15 materials support the existence of different states of water inside the pores as well: free water in completely filled regions and a film of water in a bound layer at the pore wall which coexists with the free water below a complete filling.[32]

Therefore it is assumed that the picture of the layered structure of water can be also applied for the investigated nanoporous molecular sieves. This should be especially true for the AlSBA-15 material due to the similarity of the framework structure and the nature with the MCM-41 sieve. For these reasons the low-frequency process I is assigned to water molecules forming a boundary layer at the pore surface. In addition the frequency position of this process fits rather well with that found for bound water relaxation in aerogels at the same water content (statistical thickness).[22] Process II is attributed to a second layer in which the water molecules can fluctuate more freely. The relaxation rate of the latter process is approximately 2 orders of magnitude slower that that of free water in the bulk[33] (19.2 GHz at $T =$ 298 K), but the molecules in the surface layer close to the pore walls fluctuate even much slower than those of the bulk. It must be concluded that the interaction of the water molecules with pore surface due to hydrogen bonds is quite strong.

In the following the temperature dependence of both relaxation processes will be discussed separately. In Figure 3 the relaxation rates are plotted versus inverse temperature. The low-frequency process (process I) has unusual temperature dependence. At lower temperature the relaxation rate f_p shifts to higher frequencies with increasing temperature as expected. But, reaching a certain temperature T_{max}, it decreases with further increase of the temperature. This variation of the relaxation rate can be seen already in the raw data (see Figure 2). For AlSBA-

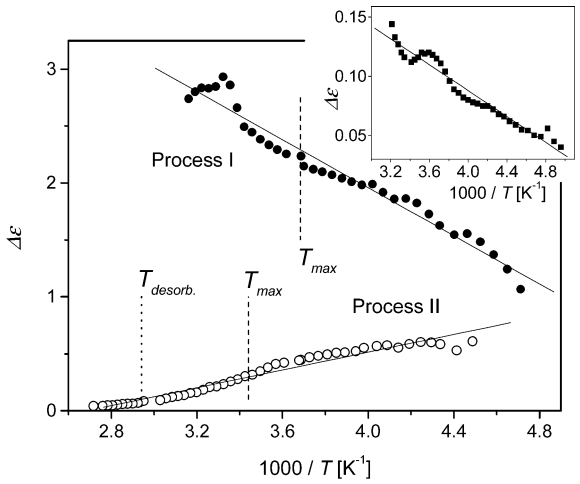

Figure 4. Dielectric strength $\Delta\epsilon$ vs inverse temperature measured for AlSBA-15: filled circles, low-frequency process I; open circles, high-frequency process II. The inset gives $\Delta\epsilon$ vs inverse temperature measured for the low-frequency process I of NMS-F. The lines are linear fits to the data.

15 a maximum value of the relaxation rate is observed at $T_{max} = 273$ K and for the NMS-F sample at $T_{max} = 280$ K. Neither the Arrhenius nor the Vogel−Fulcher−Tammann (VFT) equation[34] can be used to describe the whole temperature dependence. Such a nonmonotonic saddlelike variation of the temperature dependence of the relaxation rate is here reported for water confined to molecular sieves with large pores for the first time, in line with results found for water confined to nanoporous glasses with larger pores[13] or in the sodalite cages of faujasite.[14]

This unusual relaxation behavior cannot be related mainly to a dramatic loss of water because at the temperatures of investigation the water is close to freezing or even in a glassy state. TG measurements show a loss of mass starting from room temperature with a maximum loss at ca. 340 K, which is expected for loss of physisorbed water. But, this value is 60 K higher than T_{max}.

This conclusion is additionally supported by the temperature dependence of the dielectric relaxation strength $\Delta\epsilon$ (see Figure 4). $\Delta\epsilon$ of process I increases with temperature in the investigated temperature range and no abrupt change of this temperature dependence takes place at T_{max}. Because $\Delta\epsilon$ is proportional to the number density (the number of fluctuating dipoles per unit volume), it is expected that a loss of water should lead to a decrease of the dielectric relaxation strength rather than to the increase with temperature as it is observed. This behavior might be qualitatively understood by taking into consideration that the interaction of the water molecules with the surface of the molecular sieve is weakened with increasing temperature and more water molecules contribute to the process or/and its mean fluctuating angle (between the dipole moment and the electric field) increases with temperature.

To describe this unusual nonmonotonic temperature dependence of the relaxation time, a model developed by Feldman et al.[15] is applied. It was recently used to explain the relaxation of water in nanoporous glasses,[13] in sodalite cages of faujasite,[14] and for other confined systems.[16] In short, the nonmonotonic saddlelike behavior of this relaxation process must be due to the counterbalance of two competing processes. First, for rotational fluctuations the water molecules have to overcome energy barriers leading to Arrhenius-like temperature dependence $\sim \exp[H_a/(k_B T)]$. H_a is the height of the potential barriers between substates and k_B is the Boltzmann constant. Second, in the vicinity of a selected water molecule, a certain amount of free volume should be available for its reorientation, which can be provided by a defect. A temperature dependence of the defect concentration $\sim C \exp[-H_d/(k_B T)]$ was supposed, where H_d is the energy of the defect formation and C is the inverse maximum defect concentration. C determines mainly the value of the relaxation rate at the maximum. Subsequently, for the relaxation time (or rate) the following expression

$$\frac{1}{2\pi f_p} = \tau = \tau_\infty \exp\left[\frac{H_a}{k_B T} + C \exp\left(-\frac{H_d}{k_B T}\right)\right] \qquad (3)$$

was derived.[15]

Equation 3 was fitted to the temperature dependence of the relaxation time of process I (see Figure 3). The estimated parameters are given in the Table 2 along with the values for related systems. The maximum number of defects per mole of adsorbed water is estimated to be in the range of $10^{18}-10^{19}$. This value is much higher than in bulk ice but comparable with that found for water confined to nanoporous glasses.[15] This might suggest that more defects can be formed in water adsorbed in the nanoporous molecular sieves than in bulk ice. The values of τ_∞ for water in nanoporous molecular sieves under investigation (with hexagonal or foamlike pore structure) are smaller than those for water in porous glass.[13,15,16]

The values of the activation energy E_a (Table 2) are smaller than those found for proton hopping between neighboring Al sites in molecular sieves ($89-126$ kJ mol^{-1}), which increase in addition with increasing silica content.[24,35] These values of the activation energy might also argue against proton hopping as discussed in ref 31. Moreover especially for the NMS-F material no protons can be formed by dissociation of the SiO−H bonds under the experimental conditions, and therefore observing proton hopping is basically less probable.

In the case of the AlSBA-15 material, the temperature dependence of the relaxation rate of the relaxation process II is also saddlelike (see inset Figure 3). The Feldman model (eq 3) can be applied too to describe this complex temperature dependence. The estimated parameters are given in Table 2. The values for the prefactor and the defect concentration are higher than that for the low-frequency relaxation process I. At 298 K the value of the relaxation rate is 2 orders of magnitude lower than that of bulk water. This points to a restricted mobility even of these water molecules located in that second layer.

$\Delta\epsilon$ of the high-frequency relaxation process decreases with increasing temperature and approaches zero close to 340 K (see Figure 4). This behavior might be roughly understood by considering two processes. First, the Debye theory of dielectric relaxation predicts that the dielectric strength decreases with temperature by the relation $\Delta\epsilon \sim 1/T$. Second, TG measurements (see below) show a mass loss with a maximum rate around 340 K. This mass loss might be due to a loss of water molecules in the second layer, reducing the number density of the fluctuating dipoles for process II. This is underlined by a more careful analysis of $\Delta\epsilon(T)$, which shows that there is a change of its slope around 272 K, close to the freezing point of bulk water. This supports the hypothesis of water loss in the second layer that can take place above this temperature. It is assumed that both discussed processes contribute simultaneously to the temperature dependence of $\Delta\epsilon$.

For the NMS-F sample the relaxation rate of process II is approximately 1 order of magnitude higher than that for AlSBA-15. In the investigated temperature range an Arrhenius-like temperature dependence of f_p is observed. No unusual relaxation

TABLE 2: Fitting Parameters of the Temperature Dependence of the Relaxation Times

sample	freq range	E_a (kJ mol^{-1})	E_d (kJ mol^{-1})	log(τ_∞/s)	1/C (M^{-1})	ref
AlSBA-15	low (I)	50.8	25.4	13.0	5.8×10^{-6}	this work
AlSBA-15	high (II)	48.4	9.2	19.1	4.3×10^{-3}	this work
NMS-F	low (I)	48.1	31.3	12.8	7.7×10^{-7}	this work
NMS-F	high (II)	44.6				this work
porous glass[a]	low	55−42	39−30	13.5−12.1	9×10^{-7} to 2×10^{-5}	13, 15
Na−Y	high	19.6	22.6		0.8×10^{-2}	14

[a] Pore size from (50−70) to (280−400) nm.

behavior such as that for SBA-15 is found in the available frequency window. Fitting the Arrhenius law to the data gives the activation energy of 44.6 kJ mol^{-1}, which correlates well to values found for the so-called first relaxation process in porous glass and in bulk ice.[15] Qualitatively, it might represent twice the energy of a hydrogen bond (cited in ref 36), meaning that two such bonds have to be broken to enable the rotational and translational fluctuations of the water molecules. However, the estimated prefactor is quite high. In addition, the extrapolation of this linear temperature dependence to 298 K gives a value of 65 GHz for the characteristic frequency, which is essentially higher than that of free bulk water.[33] These facts might support the speculation that a saddlelike temperature dependence of relaxation rate—found to be characteristic for water confined to nanoporous systems—also takes place for the NMS-F sample at frequencies higher than 1 GHz, which is the highest experimentally accessible value.

A still open question is the nature of the defects in these systems. For water and ice, the nature of orientation defects is complex,[37] involving pairs of neighboring O···O atoms not bonded by hydrogen bonds or pairs of OH groups facing each other OH···HO, depending on the microscopic environment of the defect. A jump of a defect to a new site occurs by a 120° rotation of a water molecule. In the case of water confined to porous systems, despite the suppression of forming tetrahedral hydrogen bonds, there are even more possibilities to form defect sites, probably due to the presence of the framework of OH groups. The pore/cavity structure might play an important role as well.

Thermogravimetric Measurements. Representative TG curves and their derivatives are given in Figure 5A,B, respectively, for the same samples measured by dielectric spectroscopy. A similar behavior is observed for all samples: there are steps or peaks due to the loss of water, which is either physisorbed, chemisorbed, or resulted from dehydroxylation processes. It is beyond the aim of the paper to discuss these steps in TG curves in more detail because there is a bulky body of literature related to similar topics. However, the amount of water released on each step of the curve must be considered. It results that the samples were not saturated with water before the measurements.

The estimated amount is more than 10 times less than the maximum loading, while the pore filling is 0.09 for AlSBA-15 and 0.03 for NMS-F, and the estimated thickness of the water layer (if it is uniformly distributed) is 0.13 and 0.10 nm, respectively. Under these conditions, one cannot speak about the presence of bulk water: Moreover, a layer of ca. 0.4 nm was found to be nonfreezable on the pore surface of silica MCM-41 materials.[38]

Up to a certain point, DTG curves might be roughly regarded as temperature-programmed desorption (TPD) curves. These indicate one main process of mass loss for all investigated nanoporous molecular sieves. The peak observed at 340 K is due to loss of physisorbed water. To have a comparison, it should be mentioned that the main desorption maximum of water confined to faujasite is observed[14] at 385 K, while that of AlMCM-41 appears at 347 K. However, the peak of investigated nanoporous molecular sieves is asymmetrical. This gives some evidence that more than one water species might be present, having a desorption maximum around 340 K. This interpretation of the DTG data is in full agreement with the dielectric results. Unfortunately these components cannot be individually resolved even by decreasing the heating rate to 2 K min^{-1}. At temperatures higher than 600 K, water desorption is rather low, but continuous. It is due to dehydroxylation and, probably, to the partial destroying of the framework.

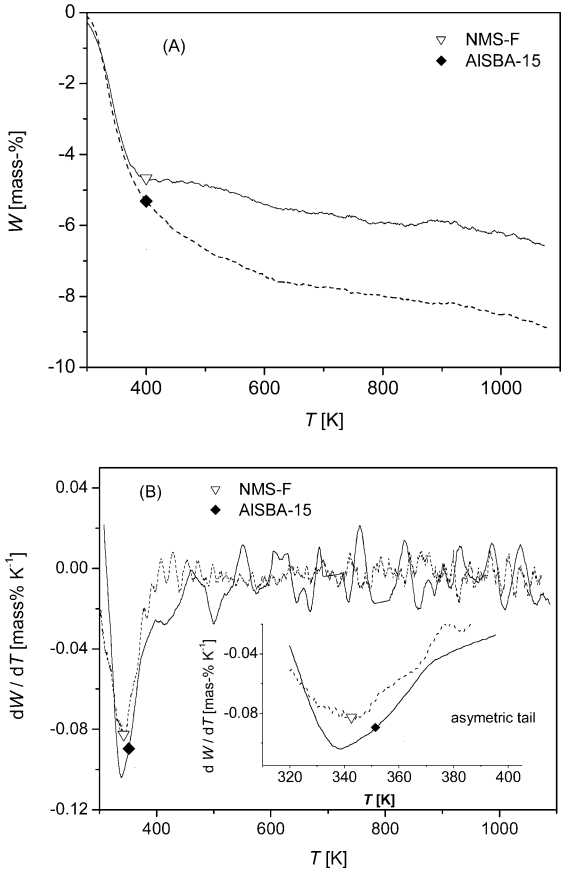

Figure 5. TG (A) and DTG (B) curves for the investigated samples of nanoporous molecular sieves. W is the symbol of the weight loss.

Conclusions

The molecular dynamics of water in the SBA-type molecular sieves was investigated by broadband dielectric spectroscopy in a large temperature range. Besides conductivity and Maxwell−Wagner−Sillars effects, two relaxation processes have been observed which are separated by 7 orders of magnitude in the frequency scale. Both of these processes are assigned to rotational fluctuations of water molecules.

The relaxation region at lower frequencies (process I) is assigned to molecules forming a surface layer close to the pore

wall. Due to the strong interaction of the water molecules with the surface OH groups by hydrogen bonds, its molecular dynamics is dramatically slowed compared to that of bulk water. The relaxation process above 1 MHz (process II) is related to water molecules forming a second layer located closer to the center of the pores.

The relaxation rates or times of process I have an unusual saddlelike temperature dependence characterized by maximum temperature T_{max}. This is found to be characteristic for water confined to nanopores. Such a saddlelike variation of the relaxation time with temperature is reported for molecular sieves with large pores for the first time. This unusual temperature dependence cannot be due to a loss of water at temperatures where the bulk water is (almost) frozen. This is supported by TG measurements showing a mass loss at quite higher temperatures than T_{max}. Moreover the temperature dependence of the dielectric relaxation strength shows no anomaly at T_{max} and increases with temperature. A loss of water should rather lead to a decrease of the dielectric relaxation strength.

For water in AlSBA-15, the temperature dependence of the relaxation time for process II also shows a saddlelike behavior, while for the NMS-F material the temperature dependence is Arrhenius-like in the accessible frequency window. It was speculated however that a saddlelike temperature dependence occurs at higher frequencies.

The saddlelike nonmonotonic variation of the relaxation times with temperature seems to be a general feature of water relaxation under confinement conditions. To describe the temperature dependence of the relaxation time, a model was used, involving the counterbalance of two competing processes: orientational fluctuations of the water molecules and the defect formation in the vicinity of water molecules. The rotation of a molecule always involves the breaking of hydrogen bonds to reach other sites.

Acknowledgment. The authors gratefully acknowledge the financial support under Schwerpunktprogramm 467 "Nanostrukturiete Wirt/Gast-Systeme" by Deutsche Forschungsgemeinschaft and thank Dr. M. M. Pohl (ACA, Berlin) for TEM pictures. L.F. and S.F. are thankful for the financial support of the Romanian Ministry of Research (Project CERES 59/C2).

References and Notes

(1) Beck, J. S.; Vartuli, J. C.; Roth, W. J.; Leonowicz, M. E.; Kresge, C. T.; Schmitt, K. D.; Chu, C. T. W.; Olson, D. H.; Sheppard, E. W.; McCullen, S. B.; Higgins, J. B.; Schlenker, J. L. *J. Am. Chem. Soc.* **1992**, *114*, 10834.

(2) (a) Zhao, D.; Huo, Q.; Feng, J.; Chmelka, B. F.; Stucky, G. D. *J. Am. Chem. Soc.* **1998**, *120*, 6024. (b) Zhao, D.; Feng, J.; Huo, Q.; Melosh, N.; Fredrickson, G. H.; Chmelka, B. F.; Stucky, G. D. *Science* **1998**, *279*, 5548. (c) Yang, P.; Zhao, D.; Margolese, D.; Stucky, G. D. *Nature* **1998**, *396*, 152. (d) Schmidt-Winkel, P.; Luckens, W. W., Jr.; Zhao, D.; Yang, P.; Chmelka, B. F.; Stucky, G. D. *J. Am. Chem. Soc.* **1999**, *121*, 254. (e) Bagshaw, S. A.; Prouzet, E.; Pinnavaia, T. J. *Science* **1995**, *267*, 865.

(3) (a) Miyazawa, K.; Inagaki, S. *Chem. Commun.* **2000**, *2121*. (b) Van Der Voort, P.; Ravikovitch, P. I.; De Jong, K. P.; Benjelloun, M.; Van Bavel, E.; Janssen, A. H.; Neimark, A. V.; Weckhuysen, B. M.; Vansant, E. F. *J. Phys. Chem.* B **2002**, *106*, 5873. (c) Yuan, Z.-Y.; Su, B. *Chem. Commun.* **2002**, 504.

(4) (a) Corma, A. *Chem. Rev.* **1997**, *97*, 2373. (b) Brunel, D. *Microporous Mesoporous Mater.* **1999**, *27*, 329.

(5) Moller, K.; Bein, T. *Chem. Mater.* **1998**, *10*, 2950.

(6) Tun, Z.; Mason, P. C.; Mansour, F. K.; Peemoeller, H. *Langmuir* **2002**, *18*, 975, and references cited herein.

(7) Takahara, S.; Nakamoto, M.; Kittaka, S.; Kuroda, Y.; Mori, T.; Hansana, H.; Yamaguchi, T. *J. Phys. Chem.* **1999**, *103*, 5814.

(8) (a) Morineau, D.; Casas, F.; Alba-Simionescu, C.; Grossman, A.; Bellissent-Funel, M. C. *J. Phys. IV* **2000**, *10*, Pr7-95. (b) Morineau, D.; Xia, Y.; Alba-Simionescu, C. *J. Chem. Phys.* **2002**, *117*, 8966.

(9) Hwang, D. W.; Sinha, A. K.; Cheng, C. Y.; Yu, T. Y.; Hwang, L. P. *J. Phys. Chem. B* **2001**, *105*, 5713.

(10) (a) Frunza, S.; Schönhals, A.; Frunza, L.; Zubowa, H.-L.; Kosslick, H.; Carius, H. E.; Fricke, R. *Chem. Phys. Lett.* **1999**, *307*, 167. (b) Frunza, S.; Frunza, L.; Schönhals, A. *J. Phys. IV* **2000**, *10*, Pr7-115.

(11) Frunza, L.; Frunza, S.; Schönhals, A.; Zubowa, H.-L.; Kosslick, H.; Fricke, R. *J. Mol. Struct.* **2000**, *563*−*564*, 491.

(12) (a) Frunza, L.; Frunza, S.; Schönhals, A.; Bentrup, U.; Fricke, R.; Pitsch, I.; Kosslick, H. *Stud. Surf. Sci. Catal.* **2002**, *142*, 1323. (b) Frunza, L.; Kosslick, H.; Bentrup, U.; Pitsch, I.; Fricke, R.; Frunza, S.; Schönhals, A. *J. Mol. Struct.* **2003**, *651*−*653*, 341. (c) Frunza, L.; Schönhals, A.; Frunza, S.; Pitsch, I.; Kosslick, H. Manuscript in preparation.

(13) (a) Gutina, A.; Axelrod, E.; Puzenko, A.; Rysiakiewicz-Pasek, E.; Kozlovich, N.; Feldman, Yu. *J. Non-Cryst. Solids* **1998**, *235*−*237*, 302.

(14) Frunza, L.; Kosslick, H.; Frunza, S.; Schönhals, A. *J. Phys. Chem. B* **2002**, *106*, 9191.

(15) Ryabov, Ya; Gutina, A.; Arkhipov, V.; Feldman, Yu. *J. Phys. Chem. B* **2001**, *105*, 1845.

(16) Ryabov, Y. E.; Puzenko, A.; Feldman, Yu. *Phys. Rev. B* **2004**, *69*, 014204.

(17) (a) Pitsch, I.; Kuerschner, U.; Mueller, D.; Parlitz, B.; Schreier, E.; Trettin, R.; Bertram, R.; Gessner, W. *J. Mater. Chem.* **1997**, *7*, 2469. (b) Pitsch, I.; Kosslick, H.; Müller, D.; Berndt, H.; Bentrup, U. *14. Deutsche Zeolith Tagung, Book of Abstracts*; Frankfurt am Main, Mar 6−8, 2002, RR3.

(18) Kim, S. S.; Pauly, T. R.; Pinnavaia, T. J. *Chem. Commun.* **2000**, 1661.

(19) Kosslick, H.; Mönnich, I.; Paetzold, E.; Oehme, G.; Fricke, R. *Microporous Mesoporous Mater.* **2001**, *44*−*45*, 537.

(20) (a) Schönhals, A.; Kremer, F.; Schlosser, E. *Phys. Rev. Lett.* **1991**, *67*, 999. (b) Kremer, F.; Schönhals, A. Broadband dielectric measurement techniques (10^{-6} Hz to 10^{12} Hz). In *Broadband Dielectric Spectroscopy;* Kremer, F., Schönhals, A., Eds.; Springer-Verlag: Berlin, 2002; pp 35−57.

(21) (a) Schlosser, E.; Schönhals, A. *Colloid Polym. Sci.* **1989**, *267*, 963. (b) Schönhals, A.; Kremer, F. Analysis of dielectric spectra. In *Broadband Dielectric Spectroscopy;* Kremer, F., Schönhals, A., Eds.; Springer-Verlag: Berlin, 2002; pp 59−98.

(22) Hench, L. L.; West, J. K. *Chem. Rev.* **1990**, *90*, 33, and references herein.

(23) da Silva, A.; Donoso, P.; Aergerter, M. A. *J. Noncryst. Solids* **1992**, *145*, 168.

(24) Simon, U.; Franke, M. E. *Microporous Mesoporous Mater.* **2000**, *41*, 1.

(25) Rozanski, S. A.; Stannarius, R.; Groothues, H.; Kremer, F. *Liq. Cryst.* **1996**, *20*, 59.

(26) Cramer, Ch.; Cramer, Th.; Arndt, M.; Kremer, F.; Naji, L.; Stannarius, R. *Mol. Cryst. Liq. Cryst.* **1997**, *303*, 209.

(27) Aliev, F. M.; Sinha, G. *Mater. Res. Soc. Proc.* **1996**, *411*, 1252.

(28) Frunza, L.; Kosslick, H.; Frunza, S.; Fricke, R.; Schönhals, A. *J. Non-Cryst. Solids* **2002**, *307*−*310*, 503.

(29) (a) Arndt, M.; Stannarius, R.; Groothues, H.; Hempel, E.; Kremer, F. *Phys. Rev. Lett.* **1997**, *79*, 2077. (b) Richert, R.; Yang, M. *J. Phys. Chem. B* **2003**, *107*, 895. (c) Arndt, M.; Stannarius, R.; Gorbatschow, W.; Kremer, F. *Phys. Rev. E* **1996**, *54*, 5377.

(30) Schönhals, A.; Rittig F.; Kärger J. Manuscript in preparation.

(31) Pissis, P.; Laudat, J.; Daoukaki, D.; Kyritsis, A. *J. Non-Cryst. Solids* **1994**, *171*, 201.

(32) Schreiber, A.; Ketelsen, I.; Findenegg, G. H. *Phys. Chem. Chem. Phys.* **2001**, *3*, 1185.

(33) Chan, R. K.; Davidson, D. W.; Whalley, E. *J. Chem. Phys.* **1965**, *43*, 2376.

(34) Kremer, F.; Schönhals, A. The scaling of the dynamics of glasses and supercooled liquids. In *Broadband Dielectric Spectroscopy*; Kremer, F., Schönhals, A., Eds.; Springer-Verlag: Berlin, 2002; pp 99−129.

(35) Franke, M. E.; Simon, U. *Solid State Ionics* **1999**, *118*, 311.

(36) Heibel, A.; Nimtz, G.; Pelster, R.; Jaggi, R. *Phys. Rev. E* **1998**, *57*, 4838.

(37) Podeszwa, R.; Buch, V. *Phys. Rev. Lett.* **1999**, *83*, 4570.

(38) Morishige, K.; Iwasaki, H. *Langmuir* **2003**, *19*, 2808.